Summer 2024

Investigation of the Relationships between Hydraulic, Physical, and Biological Soil Parameters at a Vineyard in Saint James, Missouri

Lyndsey Bennett
Missouri University of Science and Technology

Department:

INVESTIGATION OF THE RELATIONSHIPS BETWEEN HYDRAULIC, PHYSICAL, AND BIOLOGICAL SOIL PARAMETERS AT A VINEYARD IN SAINT JAMES, MISSOURI

by

LYNDSEY RAYMOND BENNETT

A THESIS

Presented to the Graduate Faculty of the

MISSOURI UNIVERSITY OF SCIENCE AND TECHNOLOGY

In Partial Fulfillment of the Requirements for the Degree

MASTER OF SCIENCE IN GEOLOGICAL ENGINEERING

2023

Approved by:

Katherine Grote, Advisor
Melanie Mormile
Jeffrey Cawlfield

ABSTRACT

Soil is a living, dynamic system that performs vital functions such as crop production, organic matter decomposition, and the flow and transport of water. Given the pressures of food and in some locales water security, climate change, and sustainability, farmers, scientists, and other related specialists and stakeholders must have access to understandable soil health indicators as well as the soil hydraulic function parameters to maximize crop growth while maintaining soil health. Although biological and physical soil parameters are different, we aim to evaluate their relationship at the field scale. Hydraulic conductivity in the vadose zone may be especially important, as it affects the flow of air and water that control many biological and chemical processes. This study makes use of recent advancements in mapping hydraulic conductivity using ground-penetrating radar techniques in a vineyard in St. James, Missouri. These maps were used to select sample locations of varying hydraulic conductivity, which was used in turn to acquire other soil parameters that are indicative of the biotic system, specifically the microbial activity and carbon cycle. This study observed that the soil health parameters strongly positively correlated with the hydraulic parameters, but neither correlated with the particle size analysis of the soil. This suggests that hydraulic conductivity is tied to the carbon cycle. We also investigated the potential for estimating soil parameters that are more difficult or expensive to measure, such as the field saturated hydraulic conductivity and soil respiration, using soil parameters that are easier or cheaper to measure, such as aggregate stability, soil organic carbon content, and bulk density. Adjusted bulk density and soil organic carbon were strong predictors of hydraulic conductivity.

ACKNOWLEDGMENTS

This opportunity would not have been possible had it not been for accepting an invitation to join a friend for a celebration at Lane Spring Park in Rolla, Missouri. The introduction to Dr. Katherine Grote, my future advisor, opened the door to building the confidence and understanding to build and deliver this project. Your support and encouragement, your friendship and compassion, your dedication to education and science are admirable traits that I hope to emulate. You've touched my life and changed my path in a way that I have yet to fully conceive. Thank you.

To my wonderful father, James B. Bennett. Your continued guidance, support, and existence have always fueled my interest in nature, science, and education. In retirement, you have been dedicated to your community and serving all within it, including the pond weeds and delicate ecosystems of the ponds and local lakes. That active citizen science and community involvement inspires me and fills my heart with pride and love. It is you that provided me with the candle in the dark always taking us as girls out on nature walks and pointing out all the beauty and life that surrounds us. You remind me that we are all connected, to challenge the status quo, that nothing in life is linear, and that all the good stuff in life is in the little things.

To Mr. Ousman Diallo, Veteran Vocational Education Coordinator, VBA VR&E. Warm regards and gratitude for your continued support and your dedication to veterans. Your professionalism and understanding, enthusiasm, and encouragement have been key to this success. I will always be indebted to the support specialists dedicated to those who serve our country. Thank you for answering the call and for believing in me.

TABLE OF CONTENTS

Page

LIST OF ILLUSTRATIONS

Page

LIST OF TABLES

Page

NOMENCLATURE

Symbol	Description
Θ_{grav}	Gravimetric water content
Θ_{vol}	Volumetric water content
Θ_{FC}	Field capacity
Θ_{PWP}	Permanent wilting point
Θ_{AWHC}	Plant available water holding capacity
D_b	Adjusted bulk density
K_{sat}	Saturated hydraulic conductivity

1. INTRODUCTION

1.1. MOTIVATION

The approach to defining soil health depends on the application. In agriculture, the soil is of the utmost importance, and extensive studies have been performed on the soil characteristics most related to crop yield. Other industries, such as horticulture and forestry, study slightly different aspects of soil. In geotechnical engineering, other aspects of soil are still considered, especially the strength and plasticity of soils. In all of these industries, soil health as it relates to ecosystem functioning and carbon sequestration is also now being considered, although this was less true historically.

Although industries consider the soil in different ways and measure different soil parameters, all industries struggle with characterizing heterogeneous soil environments using just a few measurements. Measuring soil properties can be expensive and time-consuming, and the heterogeneity of natural soil environments creates further challenges (Fetter, 1994; Longpierre et al., 2021; Nimmo et at., 2002), as measurements acquired in one location may not be representative of the system as a whole. In this research, we explore new methods of characterizing soils with limited input information, with the overall goal of making soil characterization less expensive and more effective. Because of the current challenge of feeding an expanding global population, we have chosen to focus on the characterization of agricultural soil parameters.

1.2. REVIEW OF SOIL HEALTH ASSESSMENT TOOLS

Soil is a dynamic and living, complex system that is often defined in terms of its physical, hydraulic, biological, and chemical properties. Because of the variety of fields impacted by soil, several different evaluations of soil health have been suggested, and the process of developing metrics for soil health is ongoing (Bagnall et al., 2022; Flynn et al., 2019; Norris et al., 2020; Mikha, 2004). A description of some of the most used soil health assessment tools is given below.

1.2.1. Soil Management Assessment Framework (SMAF). The Soil Management Assessment Framework was developed collaboratively with the U.S. Department of Agriculture (USDA), Agricultural Research Service (ARS), and Natural Resource Conservation Service (NRCS) to produce a soil health index relevant to agriculture (Andrews, S. et al., 2004). The SMAF has been traditionally utilized by government-funded agricultural projects. This approach includes eleven indicators for soil health, including macroaggregate stability, bulk density, electrical conductivity (and/or salinity), pH, Na-absorption ratio (used mainly in naturally high sodium soils), extractable P and K, soil organic carbon (SOC), microbial biomass (MBC), potentially mineralizable nitrogen (PMN), and ß-glucosidase enzyme assay.

1.2.2. Cornell's Comprehensive Assessment of Soil Health (CASH). Cornell has developed their own well-established comprehensive soil health manual that modifies traditional methods of analysis and is utilized in contemporary studies (Schindelbeck, R.R. et al., 2017; Moebius-Clune, B.N. et al., 2016). These parameters are categorized in different packages developed for different users of their lab services and assessment approach. Their "basic" package includes soil pH, organic matter, modified

extractable P, K, and micronutrients, as well as wet aggregate stability, active carbon, total carbon, and total nitrogen, and suggest a penetrometer reading. Their "standardPLUS" package includes all of the parameters from the basic packages as well as soil texture, soil respiration, autoclave-citrate extractable (ACE) protein, and predicted available water capacity. Most of the programs that used the CASH are state-wide or regional, but their method and comprehensive approach are cited broadly.

1.2.3. Haney's Soil Health Test (HSHT). The Haney Test for Soil Health was developed by Rick Haney for the USDA-ARS. This test measures and estimates the plant's available nutrients and its interpretation guides agronomists and farmers in fertilizer application. The tool includes measurements for inorganic N, P, and K and estimates the mineralizable N and P, water extractable organic carbon (WEOC) and nitrogen (WEON), and soil respiration (Haney et al., 2018). This tool has been implemented in recent efforts to track changes in soil health with management practices, but the results expressed high variability with suggestions for further evaluation (Sherbine et al., 2023; Singh et al., 2020).

1.2.4. North American Project to Evaluate Soil Health Measurements (NAPESHM). The North American Project to Evaluate Soil Health Measurements (NAPESHM) Project is a collaborative effort initiated in 2019 with the core goals of identifying and comparing methods of measuring the soil condition at long-term soil health agricultural management research locations. To this end, the project evaluated modern soil health tools as well as new technologies. After identifying the sites and cooperators, they implemented standardized soil measures and sampling procedures at 124 experimental sites across continental North America to measure over twenty

different soil parameters and methods listed in Table 1.1. These measurements were linked with their soil properties and the land management history, as well as the ecosystem function and services (Norris et al., 2020).

Table 1.1 NAPESHM Parameters

Property	**Indicator**	**Method**
Soil physical	Soil texture	Pipette method
	Bulk density (D_b)	Core method (7.6 cm diameter, 7.6cm depth)
	Aggregate stability	Wet sieve method and a new smartphone app method, SLAKES
	Water content, Θ_{FC} Θ_{PWP} Θ_{AWHC}	A suction method with porous ceramic plates on both intact and repacked cores at -33kPa and -1500kPa of pressure
	Soil stability index	Combination of wet and dry sieving at multiple sieve mesh sizes
	Saturated hydraulic conductivity	Two-ponding head method; Saturo device by Meter Co.
Soil chemical	pH	1:2 soil/water
	Electrical conductivity	1:2 soil/water
	Extractable P, K, Ca, Mg, Na, Fe, Zn, Cu, Mn	Mehich-3 extractant method when soil pH is >7.2
	Cation exchange capacity (CEC)	A sum of cations from Mehich-3 when soil pH is >7.2
	Base saturation	Calculation of cations from the Mehich-3 method when soil pH >7.2
	Sodium adsorption ratio	Saturated paste extract with inductively coupled plasma spectroscopy

Table 1.1 NAPESHM Parameters (continued)

Soil biological	Soil organic carbon	Dry combustion method (corrected for inorganic carbon if present with pressure calcimeter)
	Active carbon	Permanganate oxidizable carbon (POXC) method
	Short-term mineralizable carbon	Four-day incubation method
	Total Nitrogen	Dry combustion
	Nitrogen mineralization rate	Short-term anaerobic incubation method
	Soil protein index	Autoclaved citrate extractable method
	Enzyme assays	Assay incubation with colorimetric measurement
	Phospholipid fatty acid	Bligh-Dyer extractant method with chromatography
	Genomic sequencing	16rRNA, ITS, and shotgun metagenomics methods
Other	Reflectance	Vis/NIR diffuse reflectance spectroscopy
	Crop yield	Annual plot yield report summaries

1.2.4.1. A minimum suite of soil health indicators for North American agriculture (Bagnall, D. et al., 2023).

is a publication that is derived from the NAPESHM dataset that suggests a minimum test for soil health in agriculture. That suite consists of soil organic carbon, carbon mineralization, and aggregate stability.

1.2.4.2. Selecting soil hydraulic properties as indicators of soil health: measurement response to management and site characteristics (Bagnall, D. et al., 2022). This study was built on the data derived from the NAPESHM project and recommended indicators of soil hydraulic function. In this study one Saturo, infiltrometer measurement was conducted per experimental unit and was not included in the evaluation of the data. The remaining variables that were compared in this study include particle size distribution, bulk density, field capacity, wilting point (derived via laboratory method on both repacked and intact soil cores), pH, soil organic carbon, aggregate stability, 10-year precipitation, and temperature, and categorized them based on agricultural management practice. The authors concluded that suitable indicators for hydraulic properties include field capacity of intact cores as the most direct measure, but also bulk density, organic carbon, and aggregate stability that were sensitive to management and accessible.

1.2.4.3. Carbon-sensitive pedotransfer functions for plant available water (Bagnall, D. et al., 2022). This study utilized the measurements from the NAPESHM dataset to create a new pedotransfer function for estimating permanent wilting point and field capacity. In this study, the researchers distinguished the soils between calcareous and noncalcareous and created a regression function using the input parameters of the particle size analysis and soil organic carbon to estimate the available water-holding capacity. This function is replacing the previous more tedious lab method that was used for determining water content at specific suction pressures.

1.3. SOIL PARAMETERS

Despite the range of soil health assessment tools, some parameters are important for most applications, especially agriculture and carbon sequestration. This works focuses on these parameters, which are saturated hydraulic conductivity, water content, field capacity, permanent wilting point, plant available water holding capacity, adjusted bulk density, particle size distribution, soil organic carbon, active carbon, soil respiration, and aggregate stability. These parameters can be broadly classified as relating to hydraulic parameters, physical parameters, and biological parameters. Table 1.2 classifies each of the parameters used in this study into these categories and lists the methods (laboratory or calculation) used to determine each parameter.

Table 1.2 Selected Parameters

	Parameter	**Subclassification**	**Method and Analysis**
Hydraulic parameters	Saturated hydraulic conductivity K_{sat}		Saturo by Meter Group; automated ring dual head infiltrometer method.
	Water content (grav) Θ_{grav}		Gravimetric water content analysis performed at MS&T.
	Water content (vol) Θ_{vol}		Calculated as the product of adjusted bulk density and gravimetric water content.
	Available water holding capacity, non-calcareous $\Theta_{FC, non}$ - $\Theta_{PWP, non}$	Field Capacity, noncalcareous $\Theta_{FC, non}$	Calculated using PTFs (an equation derived from multilinear regression analysis) by Excel spreadsheet.
		Permanent Wilting Point, noncalcareous $\Theta_{PWP, non}$	

Table 1.2 Selected Parameters (continued)

Physical parameters	Adjusted bulk density (D_b)		Kellogg Soil Survey Method 3B6a. Performed at MS&T.
	Particle Size Distribution:	Sand	Pipette method. Analysis performed by Mizzou Soil Health Lab.
		Silt	
		Clay	
Recalculated values	Particle size distribution, adjusted to account for gravel:	Adjusted sand	The adjusted lab reported values to account for the greater than 2mm fraction material that was quantified via the adjusted bulk density method at MS&T.
		Adjusted silt	
		Adjusted clay	
		Coarse	Simplified texture analysis of what is >63µm, to include the greater than 2mm fraction
		Finer	Simplified texture analysis <63µm
Biological indicators	Wet Aggregate Stability		Cornell method. Analysis performed by Mizzou Soil Health Lab.
	Soil Organic Carbon		Dry combustion method. Analysis performed by Mizzou Soil Health Lab.
	Permanganate-oxidizable carbon (POXC)		POXC method performed by Mizzou Soil Health Lab. Represents active carbon fraction of soil organic carbon.
	Soil Respiration		SMAF method. 4-day incubation. Analysis performed by Mizzou Soil Health Lab. Measures carbon dioxide release before and after incubation.

1.3.1. Hydraulic Parameters. The hydraulic parameters selected for this study include saturated hydraulic conductivity, water content, and available water holding capacity. These parameters help to characterize the soil water relationship.

1.3.1.1. Saturated hydraulic conductivity. In hydrogeology saturated hydraulic conductivity and water-holding capacity have been thoroughly investigated (C.W. Fetter, 1994, Usowisc and Lipiec, 2021). Soil hydraulic conductivity is the ability of soil to transmit water, or, more specifically, the ability of a porous medium to transmit or move water under nearly saturated or fully saturated conditions. Soil water is influenced by multiple compounding factors including gravity and other pressures, matric potential (a force associated with capillary and adsorptive influence), presence of solutes, soil matrix composition and size characterization, tortuosity, and interconnection of pore spaces.

Agricultural applications of soil hydraulic parameters include irrigation system design and estimating soil loss due to erosion, and are often required to monitor nutrient leaching activities, be it for regulatory efforts or cost mitigation strategies. There are multiple methods to estimate field-scale hydraulic conductivity, but they are generally time intensive and subject to variability associated with field-scale heterogeneity.

The method used to measure hydraulic conductivity for this project is the Saturo device which is a fully automated dual-head infiltrometer. Each measurement can take from 1-3 hours in the field. Operation requires installing the internal ring (optional depths) in situ. Like bulk density measurements, this often requires the use of a mallet to drive the ring into the soil to the prescribed depth (in this case 15 cm for all measurements) The device has a water bladder and times the release of water and regulates pressure to produce a measurement directly in the field.

1.3.1.2. Water content, gravimetric. Gravimetric water content is the measure of the mass of water per mass of dry soil and is expressed as a percentage.

1.3.1.3. Water content, volumetric. Volumetric water content is the measure of the volume of water per volume of soil and is expressed as a percentage.

1.3.1.4. Available water holding capacity (AWHC). AWHC, also called plant available water capacity, is a measure of the amount of water available for plant crop use. AWHC is calculated as the difference between field capacity and the wilting point. AWHC is generally expressed as volume fraction or as a depth. The permanent wilting point is the soil condition at which point there is no water available to the plant. This differs from total soil water content as some of the water is locked into pore spaces or otherwise adsorbed to particles within the soil. There is still water in the soil, but it is difficult for the roots to extract for their uptake. This is also the limit at which if no additional water is added to the system, the plants will die. The wilting point is defined in terms of the amount of water per unit weight, or unit of soil bulk volume in percentage. Field capacity is the measure of how much water a soil matrix can hold after a thorough saturation and excess water can drain freely which usually takes place 1-3 days after thorough rain or irrigation.

Until recently the common laboratory method of determining AWC was generally determined using ceramic pressure membrane plates where the undisturbed, disturbed, and composited samples were analyzed to determine water content at specific pressures (Taylor and Ashcroft, 1972). With the new NAPESHM soil project, a recent publication provided labs with the opportunity to streamline the labor-intensive pressure method and apply a calculation derived from statistical multivariate analysis (Bagnall et al., 2022).

But this method still requires the full-size particle distribution analysis that is tedious and expensive (Soil Survey Staff, 2022; ASTM D-7928; Nimmo et al., 2002).

1.3.2. Physical Parameters. The physical parameters selected to evaluate for this study include particle size analysis and bulk density.

1.3.2.1. Particle size distribution. There are many different methods of determining particle size or soil texture to assist in classifying soils (Soil Survey Staff 2022). Generally, this is a measure of the size of the grains within a sample. The structure and texture of soil directly impact the porosity and permeability of the matrix. Many methods of soil classification sieve and discard the greater than 2mm fraction, which may include gravel or organic materials. Simple soil texture analysis may distinguish only between coarse (greater than 63µm diameter particles) and finer materials (less than 63µm diameter particles). For more detailed analysis the particle size analysis will create more fractions and include finer materials distinguishing between the sizes of sands, silts, and clays within a soil sample. These methods include hydrometer, laser diffraction, and pipette to name a few. Those methods tend to be time-consuming and more expensive.

1.3.2.2. Adjusted bulk density. Bulk density is a measure of the dry mass of the soil in a known volume and is an indicator of soil compaction. In highly compacted soil preferential water channels can form when created by drying cracks in fine material, wormholes, and root casts for example. (C.W. Fetter, 1994).

1.3.3. Biological Indicators. selected for this study focused on those related to the carbon cycle. The carbon cycle is vital for the functioning of life. Soil organic carbon is of high interest both as an input parameter into the equation of soil health, but also is of high interest due to climate change and interest in carbon sequestration. It represents the

biota of the soil, but it is slow to change, which is one strong reason that it is suggested to have at least one additional carbon measure.

1.3.3.1. Aggregate stability. This parameter is related to the hydraulic functioning of soils in that microbe, fungal, and small soil-dwelling creature's excretions of saccharides, proteins, and others including glomalin are largely responsible for the glue-like adhesion of particles such as micro- and macro aggregates. Extracellular secretions are highly correlated with aggregate stability and regulation of osmotic pressure (Rieke, 2022.) This is an important consideration for erosion susceptibility and is widely used in approaches to quantifying soil health. There are multiple approaches to determining aggregate stability including the Cornell rainfall simulator method as well as the common wet sieve method (USDA TN 450-03, Soil Survey Staff 2022, Norris et al. 2020, Kemper, 1986).

1.3.3.2. Soil organic carbon (SOC). Soil organic carbon represents approximately 58 percent of soil organic matter and represents the biota of the soil including plant and animal residues, living and dead microorganisms, and root exudates. SOC is linked to many soil functions including water storage and nutrient cycling. SOC indirectly relates to the hydraulic functioning of soils but is also used to account for the living and carbon-based constituents of the soil. The SOC content changes relatively slowly due to land management practices (around 3-5 years) but is of major interest for climate change efforts as well as a vital cycle to the functioning of life (Liptzin, D. et al., 2022).

1.3.3.3. Active carbon. is the fraction of SOC that is readily available for use by the living organisms in the soil. Active carbon generally represents one to four percent of the soil's organic carbon and is much more responsive to management. The laboratory procedure used in this study to determine active carbon was permanganate oxidizable carbon (POXC) method. Recent studies have suggested that this method targets biomolecules linked with the presence of polyphenolic compounds, a class of compounds often found in plant food that includes lignin and flavonoids (Kleber et al., 2021). The active carbon POXC method has been widely adopted in soil health and agricultural monitoring (Wade, J. et al., 2020).

1.3.3.4. Soil respiration. is a measure of the amount of carbon dioxide released by soil and is also known as the carbon mineralization rate. Soil respiration includes microbial and root respiration, the release of carbon dioxide associated with the mineralization of carbonates in soil and is a general indicator of the active carbon cycle. The current practice of measuring soil respiration is either a 24-hour or four-day incubation period. The released carbon dioxide is then measured by EC, gas chromatography (GC), or titration. This methods' results are associated with "uncharacteristic extracellular polymeric substances." (Rieke et al., 2022; Soil Survey Staff, 2022; Liptzin, 2022). Note in USDA Tech Memo 450-03 that there was reported higher variability among replicates during the 24-hr method verse the 4-day. Evaluating carbon dioxide emissions with the 24-h or 4-d incubation method is not a perfect measurement of true potential carbon mineralization. This process removes a soil sample from the field then dries and disaggregates before the processing of samples in the lab. However, this method is a common measurement and has been used in many studies as

an indicator of the biotic system. Since this method requires the use of an incubator and has varying lengths of incubation, we ran multilinear regression to attempt to predict soil respiration using the other variables. Also, field-measured soil respiration is noted in possible future studies.

2. BACKGROUND

2.1. SITE BACKGROUND

2.1.1. Soil and Geologic Background. According to the NRCS Soil Survey, as viewed in Figure 2.1, there are three silt loam-based soil profiles identified over the field of interest. Those profiles include the Rosati, Hartville, and Glenstead silt loam.

Figure 2.1 NRCS Soil Survey Profile

In the north and eastern aspects of the field, it is described as the Rosati silt loam. The associated parent material of the Rosati silt loam is clayey loess over residuum weather from limestone. This material is attributed to high runoff and is described as somewhat poorly drained with a water table at 12-24 inches depth. The predominant

material identified over the central and western portions of the field of interest is the Hartville silt loam. The Hartville silt loam has parent material described as clayey colluvium. This matrix is associated with a very high run-off risk and is also characterized as somewhat poorly drained, with a water table at 12-24 inches depth. In the very southern sliver of the field of interest that borders Interstate 44 is what is described as a Glensted silt loam. The associated parent material is clayey loess over clayey residuum weathered from cherty limestone. This matrix is also identified with a high risk of runoff, attributed to poor drainage, and the water table at 6-18 inches. This aspect is also identified as being associated with moderate to high organic matter depletion (NRCS Soil Survey).

To summarize, the field of interest is a silty loam with a predisposition for runoff, erosion, and drainage impediments. A somewhat restricting layer exists around 20-22 inches as indicated from as well as the broad characteristics associated with the soil taxonomy. The water table follows along the restrictive clay layer.

Evaluating Google Maps over time there are paleodrainage channels evident over the field of interest with a particular wet weather creek visible in both the 1995 and 2002 Google satellite imagery (Figure 2.2). These channels are likely a source of variability depending on how they were backfilled. During sampling, there were issues with gravel present that were accounted for in our analysis.

Figure 2.2 Historic Satellite Imagery, 1995. 2002. and 2012 respectively (Google Earth)

2.1.2. Previous Site Work. A previous study was conducted in 2020 in the field of interest which utilized ground penetrating radar (GPR) mapping for the estimation of saturated hydraulic conductivity (Leverett, 2021). In the study, they took GPR readings using electromagnetic velocity following along ten traverses expressed in Figure 2.3, before and after a rewetting event. After which the data were converted to dielectric permittivity and then to volumetric water content. The two data sets were compared, and hydraulic conductivity was calculated from the change in estimated volumetric water content with time. The derived hydraulic conductivity was later correlated with twelve field infiltrometer readings with an R^2 of 0.86. This indicates a strong linear fit between the two providing confidence in utilizing GPR to identify areas of field scale heterogeneity potentially worthy of capturing, at least in the context of the focus of this continued research. A continuing relationship exists with the vineyard and additional analyses are planned for the future within the department to include using drones to estimate relevant parameters at the field scale.

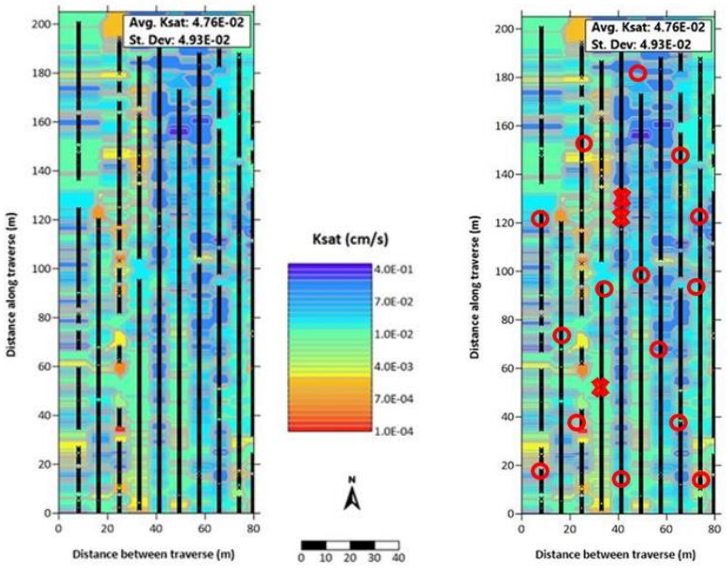

Figure 2.3 Ground Penetrating Radar (GPR) Estimated Saturated Hydraulic Conductivity at 500MHz (representing 0-18cm depth) at Vineyard in Saint James, Missouri (Leverett, 2021). Same image on right with added identified study sample sites.

2.1.3. Climate. Annual climatology information for the locale, as derived from National Weather Service Monthly Climate Normal for Vichy Airport, Missouri (1991-2020), are as follows: normal precipitation (in inches) annually 43.07, average normal temperature 55.5°F, average minimum and maximum temperature respectively, 45.3°F and 65.7°F. Over the past four years (2018-2022) monthly precipitation as reported at the same station is 41.45 inches with a minimum precipitation of 35.68 inches recorded in 2021 when the GPR data was collected.

2.1.4. Agriculture and Business. The field of particular interest supports two different varieties of grape, the Cayuga and Concord. The measurement of the field of interest is approximately 80-m x 200-m, 3.95 acres, or 1.6 hectares. Field measurements as well as measurements via satellite corroborated. There are continuous moisture probes and drain tiles installed in the rows. Harvesting had been mechanically performed

approximately two weeks before sampling began. The soil around grapevines was free of grass and the distance between canopies between the two species was slightly different (4-6 cm), which is noticeable in the satellite imagery as well as the spacing between the GPR traverse sections.

St. James Winery and the associated vineyard have been established since the 1970s. The business process, produce and bottle a variety of wines. While some of the grapes are harvested at the vineyard where the field of interest was located, some of the grapes used in their products are sourced from other farms. Current practices include mechanical harvesting and annual fertilizer application. The diatomaceous earth used in part of their processing is harvested for compost and applied to the fields.

3. METHODS

3.1. SAMPLE SITE SELECTION

Sample site locations were selected building from maps of estimated hydraulic conductivity derived from ground penetrating radar (GPR) in a previous study (Leverett, 2021). The sampling sites were selected utilizing recent geophysical data to express the range, attempting to capture the field's heterogeneity. Figure 2.3 shows the eighteen selected sample site locations identified for the scope of this study over the GPR data interpretation of the field of interest. Figure 3.1 shows the most recent Google satellite image with the sample site locations numbered as identified for the study.

Figure 3.1 Sample Site Map (Google Maps)

3.2. DATA ACQUISITION

The eighteen sites were each sampled in replicate using a hand auger to a depth of 15 cm. Each of the sites was also sampled in replicate using bulk density cores (cylinder volume 155 cm3) to a depth of 15 cm. The sampling campaign occurred September 14th-15th, and 18th, 2022. Soil depth was decided based on similar studies of soil health measurements for comparability (Norris et al., 2022). Additionally, this depth correlates with the GPR hydraulic conductivity estimates collected in the same field. Weather conditions during the sampling campaign were mild and mostly sunny. The grape varieties had different canopies as visible in Figure 3.1 and 3.2. The Concord variety had a most established and fuller canopy while the Cayuga variety that dominates the eastern half of the field of interest offered less shade to the immediate floor beneath the grapevines. It was also observed (see satellite image in Figures 2.1, 2.2, 3.1, and 3.2) and measured that the distance between rows was 4-6 cm less on the western half of the field where the Concord variety was established.

Figure 3.2 Picture Captured at Time of Sampling. Concord Variety (left), Dominates the Western Portion of the Field of Interest. The Cayuga Variety (right).

3.3. LAB ANALYSIS

The soil density cores were analyzed at the Missouri University of Science and Technology. Bulk density (D_b) calculation via Kellogg Soil Survey method 3B6a (Soil Survey Staff. 2022). The soils were removed from the stainless-steel cylinders and the weight of the soil was captured within three hours of sampling. This weight was recorded and then transcribed to Excel. Samples were transferred into metal oven-safe containers for oven drying at 110°C for 24 hours. The dried samples were weighed and then returned to the oven for one hour. They were then reweighed. The reweighing values were calculated for relative percent deviation to ensure a stable weight. Once confirmed, the samples were then sieved at 2 mm to remove and account for any gravel in the soil. The gravel was weighed, and data were recorded and then transcribed to Excel. The volume of the gravel was then determined based on their displacement of a known volume in a 100-mL volumetric cylinder. The gravel volumes were removed from the bulk density equation and are reported in 0.01g cm^{-3}. The bulk density of the total mass was calculated using equation (1). The procedure followed Kellogg Soil Survey method 3B6a (Soil Survey Staff. 2022).

$$Db = (dried\ weight - Gravel\ weight)/(core\ volume - (\frac{gravel\ weight}{density\ of\ gravel}) \quad (1)$$

The gravimetric water content was derived based on the initial weight of the bulk density core material mass, the field state weight, minus the dry weight of the soil sample. Calculated in Excel spreadsheet.

The volumetric water content was calculated as a product of adjusted bulk density and gravimetric water content. Calculated in Excel spreadsheet.

Pedotransfer function for volumetric water content is separated by calcareous soils, and non-calcareous soils are suggested in recent papers from data evaluated by the NAPESHM project mentioned previously (Bagnall et al., 2022).

Water content at the permanent wilting point for noncalcareous soils, (all units in 10g kg^{-1}):

$$\theta_{PWP,non} = 7.222 + 0.296Clay - 0.074Sand - 0.309SOC + 0.022(Sand\ x\ SOC) + 0.022(Clay\ x\ SOC) \quad (2)$$

Water content at field capacity for noncalcareous soils:

$$\theta_{FC,non} = 37.217 - 0.140Clay - 0.304Sand - 0.222SOC + 0.051(Sand\ x\ SOC) + 0.085(Clay\ x\ SOC) + 0.002(Clay\ x\ Sand) \quad (3)$$

Water content at the permanent wilting point for calcareous soils:

$$\theta_{PWP,calc} = 7.907 + 0.236Clay - 0.082Sand + 0.441SOC + 0.002(Clay\ x\ Sand) \quad (4)$$

Water content at field capacity for calcareous soils:

$$\theta_{FC,cal} = 33.351 + 0.020Clay - 0.446Sand + 1.398SOC + 0.052(Sand\ x\ SOC) - 0.077(Clay\ x\ SOC) + 0.011(Clay\ x\ Sand) \quad (5)$$

Five subsamples of the soil material were selected at random and exposed to 10% HCl to evaluate if there was any reaction or effervescence. There were no bubbles heard or observed on any of the tested soils. Even though the parent material is carbonate-based, we sampled near the surface (0-15cm) which is heavily influenced by input material. Both calculations for the PTFs (calcareous and non-calcareous) were evaluated in multivariate correlations, but ultimately the noncalcareous equation was selected for analysis in this paper.

Wet aggregate stability was measured using the Cornell simulated rainfall simulator method at the Mizzou Soil Health Lab. Particle size analysis was conducted using the Kellogg Soil Survey Pipette method which represents the soil matrix less than 2mm in size for characterization. Soil organic carbon was derived using the dry combustion method. Active carbon, our secondary carbon indicator, was measured using the POXC method. Soil respiration was performed using the SMAF recommended method which is a four-day incubation period that measures the release of carbon dioxide and was performed by the Mizzou Soil Health Lab.

Particle size distribution (PSD) analysis was further simplified to reflect more economical methods such as sieving or textural methods and considered the greater than 2mm fraction that is removed before analysis for water retention curve calculations. The original PSD values were used for the PTFs, but the adjusted values were used and compared in further analyses.

3.4. DATA ANALYSIS

Data were analyzed in Excel, ArcGIS Pro, and JMP. The statistical significance level was set to a 95% level of confidence ($p < 0.05$) for this study. Histogram analysis was conducted in JMP to determine distribution. Data that were non-normally distributed were transformed, then all data were normalized before analysis. Because of the number of data points and the purpose of this study, we did not remove any outliers.

Replicate samples were calculated for relative percent deviation from the original value with an acceptance criteria goal set at less than ten percent.

3.4.1. Analysis of Data and Transformation of Non-Normal Distribution. All data were consolidated in Excel, JMP, and ArcGIS Pro. Distribution analysis was conducted utilizing JMP. Distribution analysis was conducted on each parameter in JMP with the "compare all distributions" to help guide the transformation process. The particle size analysis fractions were not transformed as they represent a fraction of a whole, 100 percent of the sample. Transformations attempted include log, log normal, exponential, and SHASH transformations in Excel and JMP. Parameters were then normalized in Excel then transcribed back to JMP for further analysis.

3.4.2. Correlation Matrix. Calculated in JMP using multivariate methods. Color map created prioritizing clusters of correlated parameters.

3.4.3. Variograms for all Soil Properties. Variograms were created in ArcGIS Pro and GS+ then results were exported into Excel. The greater the range in a variogram, for a single parameter, indicates how far we can statistically and spatial interpolate data points with accuracy i.e. the range that a pair of points reach where at that point or greater, the correlation degrades or are not spatially co-relatable beyond that point. The model with the greatest spatial correlative potential is the Gaussian, but the other models include the exponential, spherical, and linear (i.e. “nugget”). The linear or nugget model suggests that there is no spatial correlation for that individual parameter.

3.4.4. Stepwise Regression Analysis. Stepwise regression was performed in JMP optimizing the p-value with mixed entrance into the model. Regression analysis allows us to evaluate the relationship between multiple variables of interest. For deciding between optional models, Mallows’ Cp was used to compare the precision of the model to choose the best fit. Mallows’ Cp is a metric that is based on ordinary least squares of the input

variables. The optimum value for Mallows' Cp is less than p+1, where p is the number of input variables in the model. The adjusted R^2 is reported for the models as the adjusted R^2 accounts for the predictors in the model that are less significant and are more appropriate for multivariate regression analysis (Silvestrini, 2018).

4. RESULTS

4.1. DATA ACQUIRED

4.1.1. Summary Statistics. The observed infiltrometer readings ranged from 0.35 ft/day to 7.73 ft/day. The average saturated hydraulic conductivity was 2.76 ft/day, and the median of 2.13 ft/day. The range for gravimetric water content was 12.5 to 21.6 percent with a mean of 18.4 percent and a median of 18.5 percent. For volumetric water content, the range was from 11.8 to 17.3 percent with a mean of 14.7 percent and a median of 14.4 percent. The range for available water holding capacity, noncalcareous, was 20.0 to 25.1 percent with a mean of 23.1 percent and median of 23.4 percent. Adjusted bulk density ranged from 1.00 to 1.37g/cm^3 with a mean of 1.26 and median of 1.27g/cm^3. Particle size distribution confirmed that the field of interest is indeed a silt-dominated matrix with the silt percent finer range of 45.3 to 72.6 percent with a mean of 66.9 and median of 68.3 percent although these values decrease when the particle size analysis is recalculated to account for the greater than 2mm fraction with a silt range of 37.7 to 71.6 percent, mean of 64.1 percent and median of 66.8 percent. With the simplified soil texture recalculation, the finer material ranged from 53 to 89.7 percent. The finer material average was 81.9 percent with a median of 83.6 percent. For the soil health indicators, the wet aggregate stability results had a range from 3 to 44 percent with a mean of 15 percent and a median of 10 percent. For soil organic carbon the range was from 1.9 to 3.5 percent with a mean of 2.5 and a median of 2.4 percent. The active carbon via POXC yielded values with a range from 603.4 to 1102.5 mg/Kg soil. The average active carbon was 810.5 mg/Kg soil, and the median was 805.4 mg/Kg soil. Finally, the

soil respiration values ranged from 0.3 to 1 mg CO_2/g soil with a mean and median of 0.6 mg CO_2/g soil.

4.1.2. Data Distribution and Transformation. After the preliminary statistic summary was conducted, skewness values were calculated, and histograms were created for each parameter to determine if the distribution was non-normal. Those that were non-normal were transformed. Those parameters include saturated hydraulic conductivity, adjusted bulk density, and wet aggregate stability.

4.1.3. Quality Control. Those replicate samples were evaluated, calculating the relative percent deviation for each replicate value with an expected or goal of less than ten percent relative percent deviation. One of the adjusted bulk density relative percent deviations was twenty percent which was due to the presence of gravel which upset the results. This location was already noted for the presence of gravel as it made the GPR and infiltrometer measurements difficult and was related to the old paleodrainage area in the field of interest. All other values were well within the established limits for the study.

4.2. CORRELATION MATRIX

The correlation matrix was created in JMP and a correlation color map was created to visualize the clustering of variables that are more related. As observed in Figure 4.1 there is a cluster of strongly positively correlated parameters that include the hydraulic parameters as well as the biological indicators, while at the opposite corner of the map with their strong positive correlation is the particle size analyses. Pairwise correlations were also conducted and discussed in Section 5.

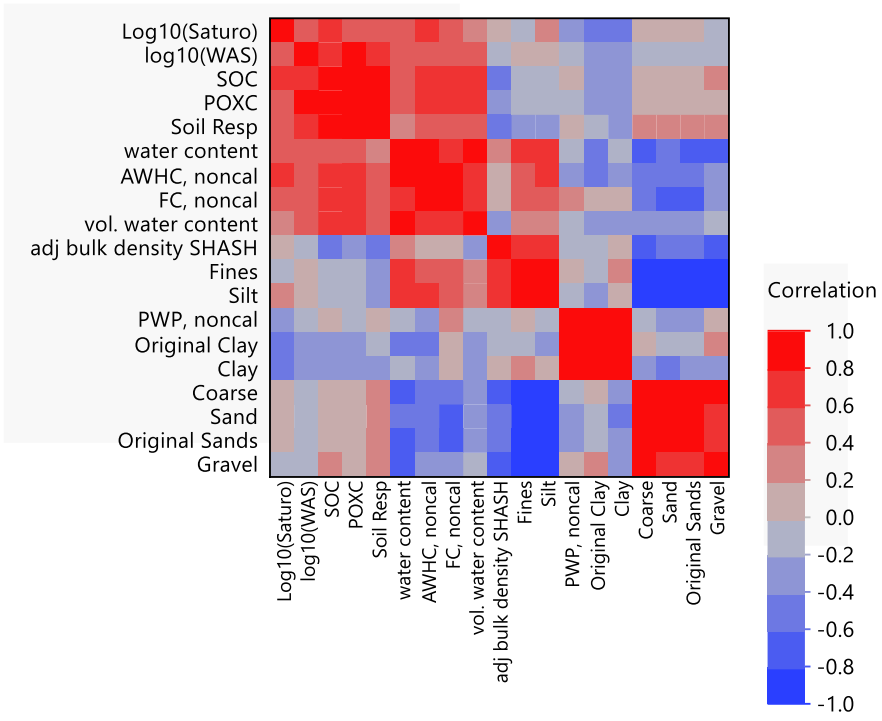

Figure 4.1 Color Map, Correlation on Clusters

4.3. VARIOGRAM ANALYSIS

Variograms were created in GS+ and then transcribed to excel for visualization. The summary of the variogram analysis for each parameter is available in Table 4.1. Many of the parameters were fitted using the Gaussian model which has a stronger spatial correlation. Some of the fitted models may not be a perfect fit and would be attributed to the inclusion of outlier data. Some parameters were found to yield linear or “nugget” models that indicate that there is no spatial correlation, no extrapolative power of the parameter based on the input data. Those parameters that were found to have linear models include adjusted bulk density, adjusted clay, and soil respiration.

Table 4.1 Variogram Summary

Variograms				
Parameter	**Sill**	**Range** (m)	**Lag** (m)	**Model Type**
K_{sat}	0.0882	45.9	85.66	Exponential
D_b	0.0857	83.8	85.66	Linear
Θ_{grav}	0.0711	8	85.66	Spherical
Θ_{vol}	0.1102	36.4	85.66	Gaussian
Original Sand	0.066	89.0	85.66	Gaussian
Original Clay	0.0618	46.1	85.66	Gaussian
Adjusted Sand	0.062	73.8	85.66	Gaussian
Adjusted Clay	0.079	83.8	85.66	Linear
$\Theta_{FC, non}$	0.0555	56.6	85.66	Gaussian
$\Theta_{PWP, non}$	0.0819	39.3	85.66	Gaussian
$\Theta_{AWHC, non}$	0.0678	61.5	85.66	Gaussian
WAS	0.1508	516.6	85.66	Exponential
SOC	0.0882	8	85.66	Spherical
POXC	0.102	66	85.66	Gaussian
Soil Respiration	0.0676	83.8	85.66	Linear

4.4. STEPWISE REGRESSION ANALYSIS

Response variable as field saturated hydraulic conductivity and independent (i.e. input) variables were adjusted bulk density, Θgrav, Θvol, SOC, active carbon, soil respiration, WAS, ΘAWHC, non, ΘFC, non, and ΘPWP, non. The results of the stepwise regression provided a model with an adjusted R2 of 0.565 that included the parameters adjusted bulk density (beta coefficient 0.69) and soil organic carbon (beta coefficient 0.9455). The resulting model has a Mallow's Cp of 3.22.

Response variable as soil respiration and the independent (i.e. input) variables included adjusted bulk density, Θgrav, SOC, active carbon, and WAS. The resulting model had an adjusted R2 of 0.84 and includes Θgrav (beta coefficient -0.135), SOC

(beta coefficient 0.38), and active carbon (beta coefficient 0.46). The Mallows Cp for the resulting model is 2.1.

4.5. KRIGING

Arc GIS Pro was used to visualize the parameters spatially using kriging. The kriging was based on the ArcGIS Pro optimization of the parameters variogram. Because this information is similar to the variograms, the only kriging included for the purpose of this study is the wet aggregate stability. The wet aggregate stability trended different from the other, highly correlated parameters in that it appeared to trend more in line with the grape species and in a north-to-south gradient orientation (Figure 4.1 and 4.2). More on this in section 5.

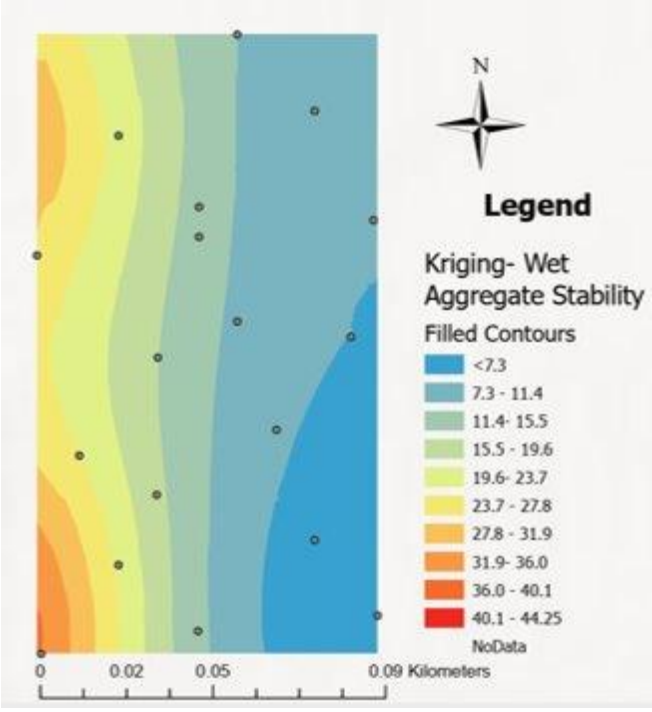

Figure 4.2 Kriging Wet Aggregate Stability

5. DISCUSSION

Before transformation parameters were uploaded to ArcGIS Pro and evaluated spatially using kriging derived from optimized semi-variograms. An interesting relationship appeared during the preliminary assessment that is that the wet aggregate stability parameter appeared to relate with the species of grape or rather that there was a dividing line down the middle of the field indicating that the dividing line between species could be the boundary (Figure 4.2). This could be investigated further as some microbes and fungi have specific plant host relationships and life cycles (Bitterlich et al., 2018), and this could be related to the canopy maturity as visualized in Figure 3.2 with field pictures of the two different grape species canopies at the time of sampling, that is also very visible on the historical satellite imagery with the delineation between varieties evident.

Saturated hydraulic conductivity correlated most strongly with soil organic carbon and available water holding capacity, noncalcareous (at 0.6534 and 0.6306 respectively). After SOC and AWHC, the next level of correlative individual parameters for K_{sat} includes WAS (0.5843), active carbon (0.5814), and soil respiration (0.5283). The last two correlations that are statistically significant include field capacity, non (0.5128), and gravimetric water content (0.5013). All of the biological indicators selected for this field correlated with the saturated hydraulic conductivity. This suggests that the observed saturated hydraulic conductivity is strongly linked to the carbon cycle.

These relationships are interesting as the primary literature review generally attribute the physical parameters for hydraulic conductivity and this study shows that, at

least at the one-on-one correlative evaluation, the biological parameters are a significant piece of the flow of water through a soil matrix. The PTF parameters correlated strongly with K_{sat} which could be a byproduct of the strong relationship with soil organic carbon, and that being a primary variable in the PTF.

Adjusted bulk density on its own correlated with the coarse or sand content, but not with any other parameters. But, when combined with the gravimetric water content to derive the volumetric water content, the correlations with soil health parameters pull through. This is strongly related to the composition of the matrix and can be indicative of compaction or the general status of the physical space within the field of interest.

Volumetric water content individually correlates strongly with available water holding capacity (0.7336), active carbon (0.6800), SOC (0.6749), field capacity (0.6492), and soil respiration (0.5830). This is likely due to the relationship with the current field conditions being closer to field capacity at the time of sampling, but also of the increase in water holding with a higher presence of carbon-related materials and organisms, and the preferential pathways that are generated in and through their life cycles. Additionally, the paleodrainage pathways provide preferential flow with the presence of larger (greater than 2mm) fragments including gravel as observed at the site that did cause some reading issues with the infiltrometer, as reported from the GPR study (Leverette, 2021).

6. CONCLUSIONS

6.1. KEY POINTS

Hydraulic conductivity was observed to range across a less than four-acre field from less than one foot per day to almost eight feet per day. Variograms express that the range for hydraulic conductivity as it relates to the spatial extrapolative interpretability was at 45.9 m (150 ft). These values suggest that to capture field scale heterogeneity it is important to take multiple measurements, or to develop new technologies and techniques to estimate hydraulic conductivity. Regression analysis suggests that of all the parameters used in this study, adjusted bulk density and soil organic carbon are strong variables in attempting to predict hydraulic conductivity (adjusted R2 0.56.)

This study found that hydraulic conductivity is strongly correlated to the biological indicators chosen for this study, (SOC, active carbon, soil respiration, and WSA), especially when compared to the physical parameters. This suggests that hydraulic conductivity is strongly related to the carbon cycle, and the biotic system of soil.

The biological indicators were observed to range across the field. The range for soil organic carbon from 1.9 to 3.5 percent. For active carbon the range was 600 to 1100mg/Kg soil. And the soil respiration observed range was 0.3 to 2 mg CO2/g soil. In evaluating the spatial correlation via variogram analysis both active carbon and soil respiration outperformed soil organic carbon with ranges of 66 m, 84 m and 8 m respectively. Because it has been reported that soil organic carbon changes slowly with

management practices, this confirms the contemporary guidance to include a secondary carbon parameter in evaluating soil health.

Soil health assessment scoring systems tend to follow one of three approaches: “more is better” (upper asymptotic sigmoid curve), “less is better” (lower asymptotic sigmoid curve), or a midpoint optimum (Gaussian function). (Andrews et al. 2004, Karlen and Stott 1994). Perhaps in evaluating and collecting comparable data, we will be able to optimize functions and relationships as they pertain to soil health, and society will have a more balanced understanding and method of measuring what soil health is.

6.2. POSSIBLE FUTURE WORK

Further studies should include metagenomic sequencing to tie these parameters to the microbial and fungal diversity and taxonomies as they are of vital importance to the aggregation of soils that directly relate to the stability of soils as well as the flow and transport of water and nutrients. Previous studies have shown the relationship with arbuscular mycorrhizal fungi with hydraulic conductivity in potted plants (Bitterlich, 2018), expanding to field scale would be an opportunity to expand the database of knowledge to understand the biotic system of soil more deeply.

Laboratory soil respiration tests are performed on dried, disaggregated, then rewetted samples. As previously mentioned, there has been higher variability reported with the 24-hour incubation method when compared to the four-day method, but finding a tool that could measure soil respiration directly in the field would be more representative of the matrix.

Also, the Meter Group has two laboratory instruments available that could be of interest for later use in evaluating methods for capturing the essential-but-nuanced hydraulic function as a variable for farmers, researchers, and policymakers in calculating soil health measurements. These include the HYRPOP 2, an all-in-one device that allows the user to sample and test undisturbed soil samples. It uses two mini-tensiometers to measure water potential while the sample air-dries, and automated balance recording create a soil moisture release curve. This same sample and the same sample ring can be used on their KSAT device that measures falling head (automated) and constant head on intact soil cores (Meter Group, n.d.).

An additional option for future studies might include additional parameters such as evapotranspiration, solar angle and/or radiation values, climatology, electric conductivity, pH, and maybe even drone derived data such as near VIS and IR data to feed a machine learning algorithm.

Elucidating the interconnectedness of the soil matrix will facilitate collaboration across fields to preserve and sustain future populations in the face of a changing climate.

APPENDIX

Table A.1 Pairwise Correlations

Variable	by Variable	Correlation	n	Lower 95%	Upper 95%	p-value
D_b	K_{sat}	0.1771	16	-0.3493	0.6185	0.5118
Θ_{grav}	K_{sat}	0.5013	16	0.0075	0.7986	0.0479*
Θ_{grav}	D_b	0.2396	18	-0.2559	0.6354	0.3383
Θ_{vol}	K_{sat}	0.3791	16	-0.1435	0.7364	0.1475
Θ_{vol}	D_b	-0.2516	18	-0.6429	0.2439	0.3139
Θ_{vol}	Θ_{grav}	0.8664	18	0.6710	0.9493	<.0001*
SOC	K_{sat}	0.6534	16	0.2333	0.8680	0.0061*
SOC	D_b	-0.4015	18	-0.7313	0.0804	0.0986
SOC	Θ_{grav}	0.4534	18	-0.0170	0.7595	0.0588
SOC	Θ_{vol}	0.6749	18	0.3038	0.8682	0.0021*
POXC	K_{sat}	0.5814	16	0.1203	0.8361	0.0182*
POXC	D_b	-0.3685	18	-0.7127	0.1189	0.1324
POXC	Θ_{grav}	0.4994	18	0.0424	0.7836	0.0348*
POXC	Θ_{vol}	0.6800	18	0.3123	0.8705	0.0019*
POXC	SOC	0.9347	18	0.8300	0.9758	<.0001*
Soil Resp	K_{sat}	0.5283	16	0.0441	0.8115	0.0354*
Soil Resp	D_b	-0.4360	18	-0.7501	0.0388	0.0705
Soil Resp	Θ_{grav}	0.3350	18	-0.1563	0.6934	0.1742
Soil Resp	Θ_{vol}	0.5830	18	0.1595	0.8252	0.0111*

Table A.1 Pairwise Correlations (continued)

Soil Resp	SOC	0.9077	18	0.7651	0.9655	<.0001*
Soil Resp	POXC	0.9080	18	0.7657	0.9656	<.0001*
WAS	K_{sat}	0.5843	16	0.1248	0.8375	0.0175*
WAS	D_b	-0.1922	18	-0.6048	0.3018	0.4448
WAS	Θ_{grav}	0.4302	18	-0.0459	0.7470	0.0748
WAS	Θ_{vol}	0.4866	18	0.0255	0.7769	0.0406*
WAS	SOC	0.7018	18	0.3495	0.8803	0.0012*
WAS	POXC	0.8468	18	0.6284	0.9415	<.0001*
WAS	Soil Resp	0.7126	18	0.3683	0.8850	0.0009*
$\Theta_{AWHC, non}$	K_{sat}	0.6306	16	0.1963	0.8581	0.0088*
$\Theta_{AWHC, non}$	D_b	0.1468	18	-0.3436	0.5743	0.5609
$\Theta_{AWHC, non}$	Θ_{grav}	0.8095	18	0.5508	0.9263	<.0001*
$\Theta_{AWHC, non}$	Θ_{vol}	0.7336	18	0.4057	0.8942	0.0005*
$\Theta_{AWHC, non}$	SOC	0.6937	18	0.3354	0.8766	0.0014*
$\Theta_{AWHC, non}$	POXC	0.6855	18	0.3215	0.8730	0.0017*
$\Theta_{AWHC, non}$	Soil Resp	0.5197	18	0.0697	0.7939	0.0271*
$\Theta_{AWHC, non}$	WAS	0.5909	18	0.1712	0.8290	0.0098*
$\Theta_{FC, non}$	K_{sat}	0.5128	16	0.0229	0.8041	0.0422*
$\Theta_{FC, non}$	D_b	0.0695	18	-0.4107	0.5195	0.7842
$\Theta_{FC, non}$	Θ_{grav}	0.6886	18	0.3267	0.8744	0.0016*

Table A.1 Pairwise Correlations (continued)

$\Theta_{FC, non}$	Θ_{vol}	0.6492	18	0.2616	0.8565	0.0036*
$\Theta_{FC, non}$	SOC	0.7034	18	0.3522	0.8810	0.0011*
$\Theta_{FC, non}$	POXC	0.6210	18	0.2171	0.8434	0.0059*
$\Theta_{FC, non}$	Soil Resp	0.5325	18	0.0873	0.8004	0.0229*
$\Theta_{FC, non}$	WAS	0.4843	18	0.0226	0.7758	0.0417*
$\Theta_{FC, non}$	$\Theta_{AWHC, non}$	0.8491	18	0.6333	0.9424	<.0001*
$\Theta_{PWP, non}$	K_{sat}	-0.3201	16	-0.7041	0.2087	0.2267
$\Theta_{PWP, non}$	D_b	-0.1340	18	-0.5655	0.3551	0.5961
$\Theta_{PWP, non}$	Θ_{grav}	-0.1605	18	-0.5837	0.3312	0.5246
$\Theta_{PWP, non}$	Θ_{vol}	-0.0980	18	-0.5401	0.3866	0.6990
$\Theta_{PWP, non}$	SOC	0.0738	18	-0.4071	0.5227	0.7709
$\Theta_{PWP, non}$	POXC	-0.0639	18	-0.5154	0.4153	0.8010
$\Theta_{PWP, non}$	Soil Resp	0.0665	18	-0.4132	0.5173	0.7932
$\Theta_{PWP, non}$	WAS	-0.1493	18	-0.5760	0.3414	0.5543
$\Theta_{PWP, non}$	$\Theta_{AWHC, non}$	-0.2017	18	-0.6110	0.2928	0.4222
$\Theta_{PWP, non}$	$\Theta_{FC, non}$	0.3461	18	-0.1440	0.6999	0.1594
Coarse	K_{sat}	0.0183	16	-0.4818	0.5094	0.9465
Coarse	D_b	-0.6603	18	-0.8616	-0.2796	0.0029*
Coarse	Θ_{grav}	-0.6374	18	-0.8510	-0.2428	0.0044*
Coarse	Θ_{vol}	-0.2485	18	-0.6410	0.2471	0.3201

Table A.1 Pairwise Correlations (continued)

Coarse	SOC	0.1606	18	-0.3311	0.5837	0.5244
Coarse	POXC	0.0957	18	-0.3885	0.5385	0.7057
Coarse	Soil Resp	0.2827	18	-0.2122	0.6622	0.2557
Coarse	WAS	-0.0270	18	-0.4877	0.4455	0.9154
Coarse	$\Theta_{AWHC, non}$	-0.4968	18	-0.7822	-0.0389	0.0360*
Coarse	$\Theta_{FC, non}$	-0.5020	18	-0.7849	-0.0459	0.0338*
Coarse	$\Theta_{PWP, non}$	-0.0473	18	-0.5031	0.4290	0.8521
Fines	K_{sat}	-0.0183	16	-0.5094	0.4818	0.9465
Fines	D_b	0.6603	18	0.2796	0.8616	0.0029*
Fines	Θ_{grav}	0.6374	18	0.2428	0.8510	0.0044*
Fines	Θ_{vol}	0.2485	18	-0.2471	0.6410	0.3201
Fines	SOC	-0.1606	18	-0.5837	0.3311	0.5244
Fines	POXC	-0.0957	18	-0.5385	0.3885	0.7057
Fines	Soil Resp	-0.2827	18	-0.6622	0.2122	0.2557
Fines	WAS	0.0270	18	-0.4455	0.4877	0.9154
Fines	$\Theta_{AWHC, non}$	0.4968	18	0.0389	0.7822	0.0360*
Fines	$\Theta_{FC, non}$	0.5020	18	0.0459	0.7849	0.0338*
Fines	$\Theta_{PWP, non}$	0.0473	18	-0.4290	0.5031	0.8521
Fines	Coarse	-1.0000	18	-1.0000	-1.0000	<.0001*
Gravel	K_{sat}	-0.1683	16	-0.6129	0.3572	0.5333

Table A.1 Pairwise Correlations (continued)

Gravel	D_b	-0.6850	18	-0.8728	-0.3207	0.0017*
Gravel	Θ_{grav}	-0.6132	18	-0.8397	-0.2051	0.0068*
Gravel	Θ_{vol}	-0.1964	18	-0.6075	0.2978	0.4348
Gravel	SOC	0.2509	18	-0.2446	0.6425	0.3153
Gravel	POXC	0.1172	18	-0.3699	0.5537	0.6433
Gravel	Soil Resp	0.3154	18	-0.1777	0.6818	0.2024
Gravel	WAS	-0.0430	18	-0.4998	0.4326	0.8655
Gravel	$\Theta_{AWHC, non}$	-0.3746	18	-0.7162	0.1119	0.1257
Gravel	$\Theta_{FC, non}$	-0.2756	18	-0.6578	0.2196	0.2684
Gravel	$\Theta_{PWP, non}$	0.1548	18	-0.3364	0.5798	0.5396
Gravel	Coarse	0.9313	18	0.8217	0.9745	<.0001*
Gravel	Fines	-0.9313	18	-0.9745	-0.8217	<.0001*
Sand	K_{sat}	0.1370	16	-0.3848	0.5925	0.6129
Sand	D_b	-0.5283	18	-0.7983	-0.0815	0.0242*
Sand	Θ_{grav}	-0.5627	18	-0.8154	-0.1300	0.0151*
Sand	Θ_{vol}	-0.2662	18	-0.6520	0.2292	0.2857
Sand	SOC	0.0360	18	-0.4383	0.4945	0.8874
Sand	POXC	0.0569	18	-0.4212	0.5102	0.8226
Sand	Soil Resp	0.2019	18	-0.2925	0.6112	0.4216
Sand	WAS	-0.0051	18	-0.4708	0.4629	0.9840

Table A.1 Pairwise Correlations (continued)

Sand	$\Theta_{AWHC, non}$	-0.5520	18	-0.8101	-0.1147	0.0175*
Sand	$\Theta_{FC, non}$	-0.6708	18	-0.8664	-0.2970	0.0023*
Sand	$\Theta_{PWP, non}$	-0.2617	18	-0.6492	0.2338	0.2942
Sand	Coarse	0.9166	18	0.7861	0.9689	<.0001*
Sand	Fines	-0.9166	18	-0.9689	-0.7861	<.0001*
Sand	Gravel	0.7079	18	0.3600	0.8830	0.0010*
Silt	K_{sat}	0.2044	16	-0.3242	0.6357	0.4477
Silt	D_b	0.6539	18	0.2692	0.8586	0.0032*
Silt	Θ_{grav}	0.7020	18	0.3497	0.8803	0.0012*
Silt	Θ_{vol}	0.3231	18	-0.1693	0.6864	0.1910
Silt	SOC	-0.0916	18	-0.5356	0.3920	0.7177
Silt	POXC	-0.0136	18	-0.4774	0.4562	0.9574
Silt	Soil Resp	-0.2256	18	-0.6265	0.2697	0.3681
Silt	WAS	0.1050	18	-0.3805	0.5452	0.6783
Silt	$\Theta_{AWHC, non}$	0.6081	18	0.1972	0.8373	0.0074*
Silt	$\Theta_{FC, non}$	0.5031	18	0.0473	0.7855	0.0333*
Silt	$\Theta_{PWP, non}$	-0.1485	18	-0.5755	0.3421	0.5566
Silt	Coarse	-0.9757	18	-0.9911	-0.9345	<.0001*
Silt	Fines	0.9757	18	0.9345	0.9911	<.0001*
Silt	Gravel	-0.9241	18	-0.9717	-0.8041	<.0001*

Table A.1 Pairwise Correlations (continued)

Silt	Sand	-0.8774	18	-0.9536	-0.6953	<.0001*
Clay	K_{sat}	-0.4322	16	-0.7642	0.0808	0.0945
Clay	D_b	0.1958	18	-0.2983	0.6072	0.4362
Clay	Θ_{grav}	-0.1122	18	-0.5502	0.3743	0.6576
Clay	Θ_{vol}	-0.2544	18	-0.6447	0.2412	0.3084
Clay	SOC	-0.3348	18	-0.6933	0.1566	0.1745
Clay	POXC	-0.3742	18	-0.7160	0.1123	0.1261
Clay	Soil Resp	-0.3154	18	-0.6818	0.1777	0.2024
Clay	WAS	-0.3257	18	-0.6879	0.1665	0.1873
Clay	$\Theta_{AWHC, non}$	-0.3473	18	-0.7006	0.1427	0.1580
Clay	$\Theta_{FC, non}$	0.1237	18	-0.3642	0.5583	0.6248
Clay	$\Theta_{PWP, non}$	0.8459	18	0.6265	0.9411	<.0001*
Clay	Coarse	-0.3588	18	-0.7072	0.1298	0.1437
Clay	Fines	0.3588	18	-0.1298	0.7072	0.1437
Clay	Gravel	-0.2685	18	-0.6535	0.2268	0.2813
Clay	Sand	-0.4009	18	-0.7310	0.0811	0.0992
Clay	Silt	0.1455	18	-0.3448	0.5734	0.5645
Original Sands	K_{sat}	0.1127	16	-0.4057	0.5762	0.6778
Original Sands	D_b	-0.5816	18	-0.8246	-0.1575	0.0114*
Original Sands	Θ_{grav}	-0.6013	18	-0.8340	-0.1869	0.0083*
Original Sands	Θ_{vol}	-0.2687	18	-0.6536	0.2266	0.2809

Table A.1 Pairwise Correlations (continued)

Original Sands	SOC	0.0571	18	-0.4210	0.5104	0.8219
Original Sands	POXC	0.0548	18	-0.4229	0.5087	0.8290
Original Sands	Soil Resp	0.2099	18	-0.2849	0.6163	0.4033
Original Sands	WAS	-0.0316	18	-0.4912	0.4418	0.9009
Original Sands	$\Theta_{AWHC, non}$	-0.5574	18	-0.8128	-0.1224	0.0162*
Original Sands	$\Theta_{FC, non}$	-0.6477	18	-0.8558	-0.2593	0.0037*
Original Sands	$\Theta_{PWP, non}$	-0.2094	18	-0.6160	0.2854	0.4044
Original Sands	Coarse	0.9565	18	0.8847	0.9840	<.0001*
Original Sands	Fines	-0.9565	18	-0.9840	-0.8847	<.0001*
Original Sands	Gravel	0.7866	18	0.5052	0.9168	0.0001*
Original Sands	Sand	0.9911	18	0.9756	0.9967	<.0001*
Original Sands	Silt	-0.9210	18	-0.9705	-0.7966	<.0001*
Original Sands	Clay	-0.3955	18	-0.7279	0.0876	0.1043
Original Clay	K_{sat}	-0.4290	16	-0.7625	0.0847	0.0973
Original Clay	D_b	-0.1357	18	-0.5666	0.3536	0.5914
Original Clay	Θ_{grav}	-0.4083	18	-0.7350	0.0724	0.0925
Original Clay	Θ_{vol}	-0.3485	18	-0.7013	0.1414	0.1564
Original Clay	SOC	-0.2071	18	-0.6145	0.2876	0.4097
Original Clay	POXC	-0.3149	18	-0.6816	0.1781	0.2031
Original Clay	Soil Resp	-0.1558	18	-0.5804	0.3355	0.5370
Original Clay	WAS	-0.3443	18	-0.6988	0.1460	0.1618

Table A.1 Pairwise Correlations (continued)

Original Clay	$\Theta_{AWHC, non}$	-0.5250	18	-0.7966	-0.0770	0.0253*
Original Clay	$\Theta_{FC, non}$	0.0028	18	-0.4647	0.4690	0.9913
Original Clay	$\Theta_{PWP, non}$	0.9376	18	0.8373	0.9769	<.0001*
Original Clay	Coarse	0.0889	18	-0.3944	0.5336	0.7258
Original Clay	Fines	-0.0889	18	-0.5336	0.3944	0.7258
Original Clay	Gravel	0.2174	18	-0.2776	0.6212	0.3861
Original Clay	Sand	-0.0664	18	-0.5172	0.4133	0.7936
Original Clay	Silt	-0.3012	18	-0.6734	0.1927	0.2245
Original Clay	Clay	0.8817	18	0.7050	0.9553	<.0001*
Original Clay	Original Sands	-0.0221	18	-0.4840	0.4494	0.9306

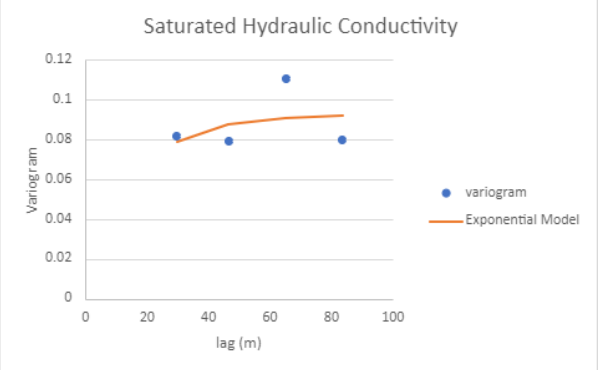

Figure A.1 Saturated Hydraulic Conductivity Variogram

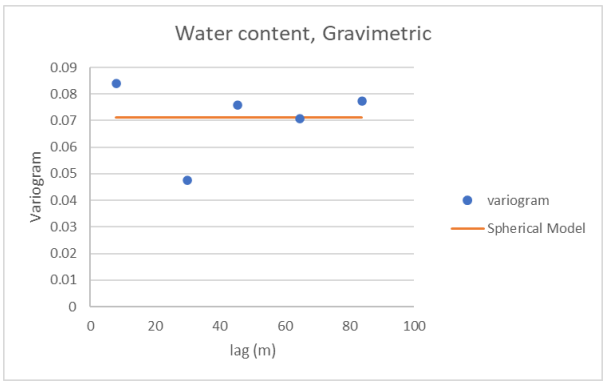

Figure A.2 Gravimetric Water Content Variogram

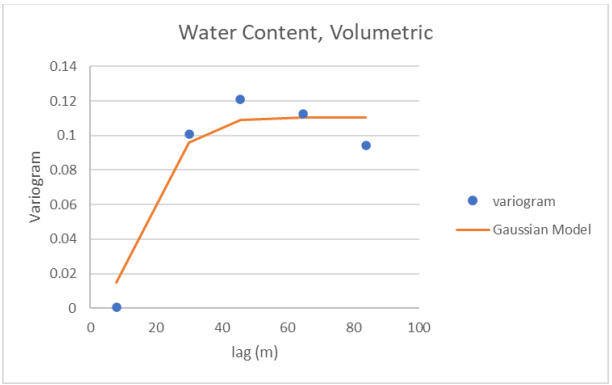

Figure A.3 Volumetric Water Content Variogram

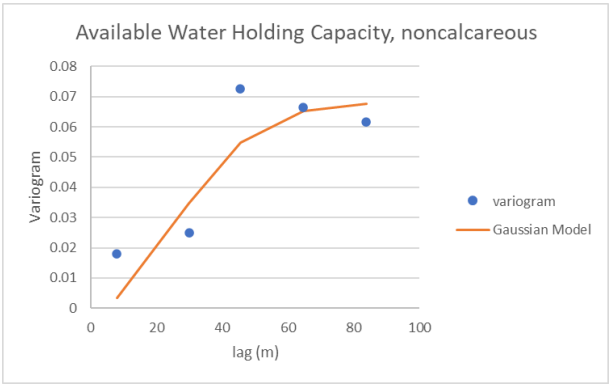

Figure A.4 Available Water Holding Capacity, noncalcareous Variogram

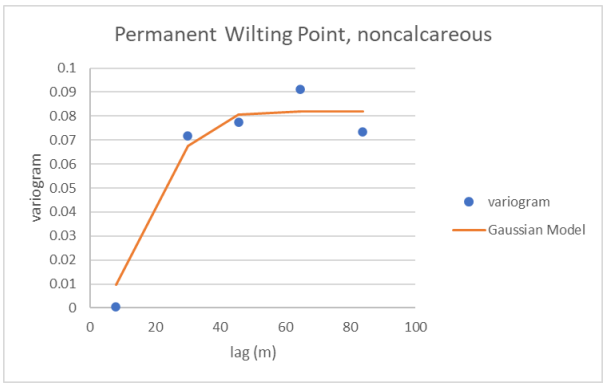

Figure A.5 Permanent Wilting Point, noncalcareous Variogram

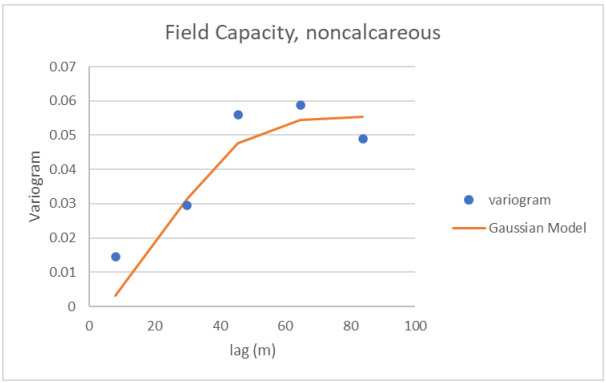

Figure A.6 Field Capacity, noncalcareous Variogram

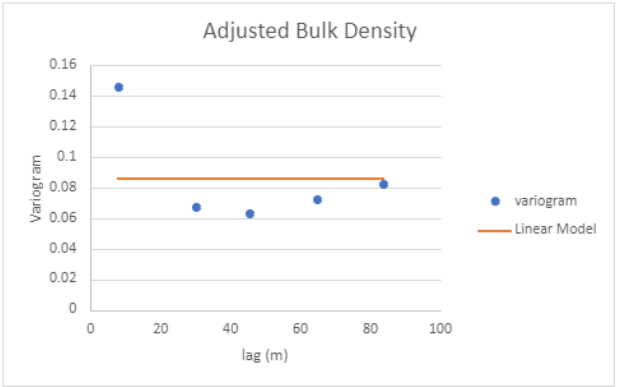

Figure A.7 Adjusted Bulk Density Variogram

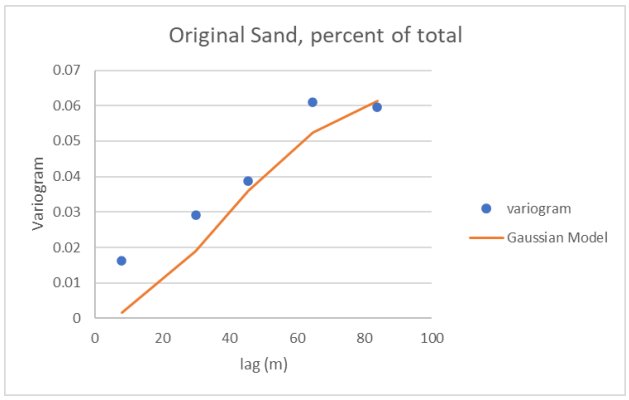

Figure A.8 Original Sand Content Variogram

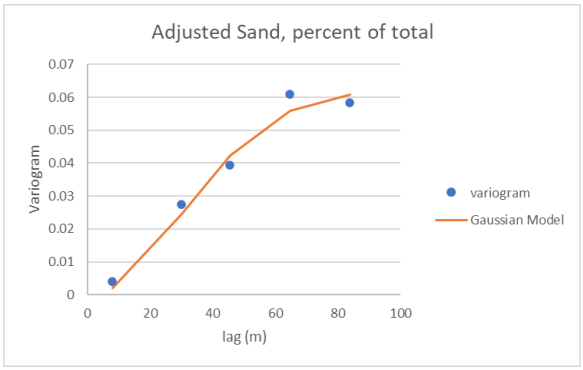

Figure A.9 Adjusted Sand Content Variogram

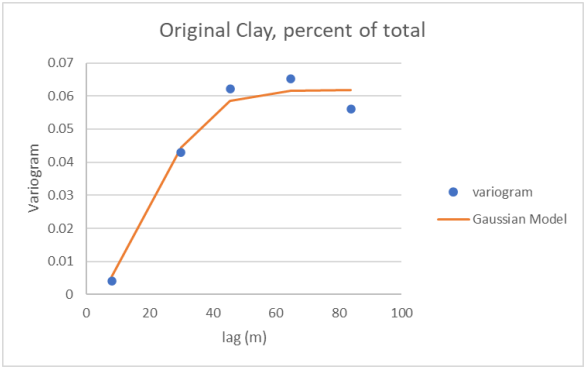

Figure A.10 Original Clay Content Variogram

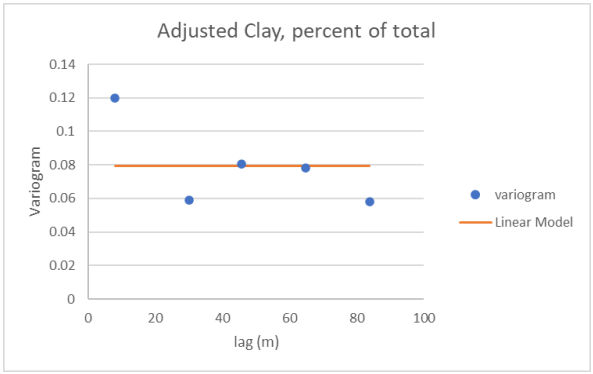

Figure A.11 Adjusted Clay Content Variogram

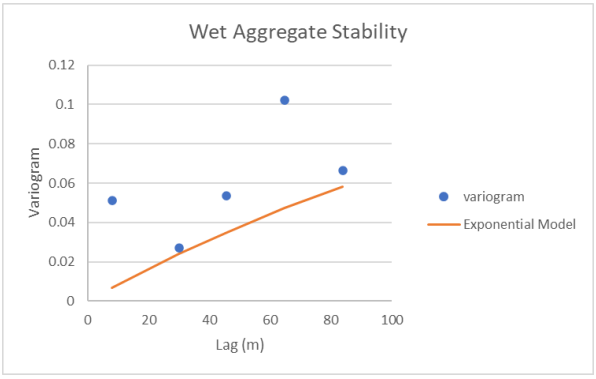

Figure A.12 Wet Aggregate Stability Variogram

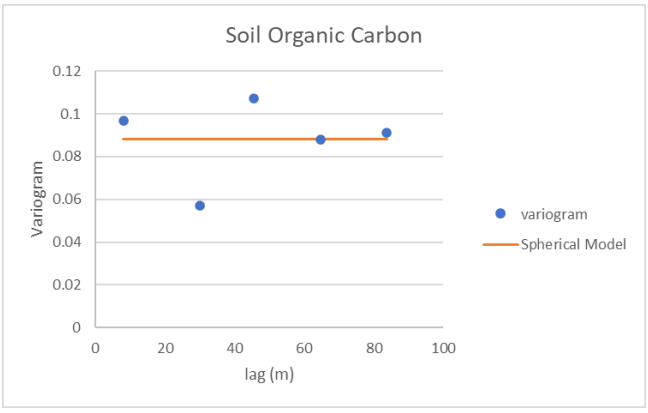

Figure A.13 Soil Organic Carbon Variogram

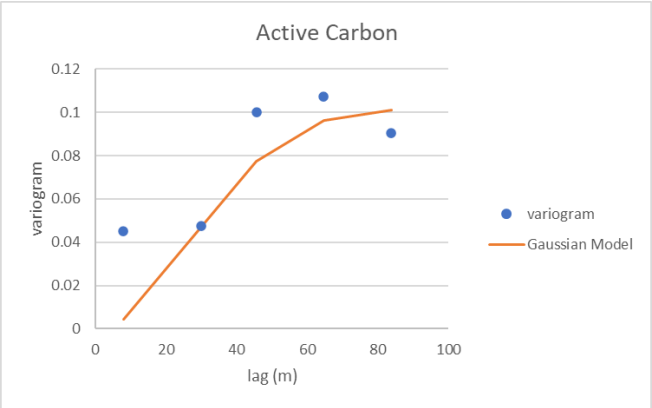

Figure A.14 Active Carbon Variogram

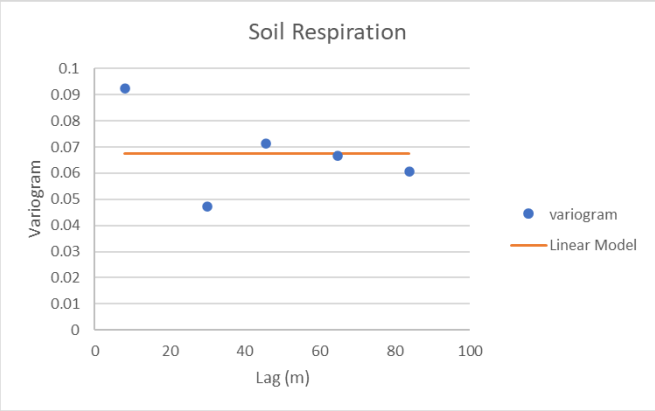

Figure A.15 Soil Respiration Variogram

BIBLIOGRAPHY

Aguilera P., Ortiz N., Becerra N., Turrini A., Gaínza-Cortés F., Silva-Flores P., Aguilar-Paredes A., Romero J. K., Jorquera-Fontena E., Mora M., Borie F. (2022). Application of Arbuscular Mycorrhizal Fungi in Vineyards: Water and Biotic Stress Under a Climate Change Scenario: New Challenge for Chilean Grapevine Crop. *Frontiers in Microbiology, 13.* DOI=10.3389/fmicb.2022.826571

Andrews, S., Karlen, D., Cambardella, C. The Soil Management Assessment Framework: A Quantitative Soil Quality Evaluation Method. *Soil Science Society of America Journal*, Madison, WI. 2004.

ASTM D6913 D7928 Particle Size Analysis, Hydrometer Method

Bagnall, D., Rieke, E., Morgan, C., Liptzin, D., Cappellazzi, S., Honeycutt, C. A Minimum Suite of Soil Health Indicators for North American Agriculture. *Soil Security*, Volume 10, 2023, 100084, ISSN 2667-0062. https://doi.org/10.1016/j.soisec.2023.100084.

Bagnall, D., Morgan, C., Cope, M., Bean, G., Cappellazzi, S., Greub, K., Liptzin, D., Norris, C., Rieke, E., Tracy, P., Aberle, E., Ashworth, A., Bañuelos Tavarez, O., Bary, A., Baumhardt, R., Borbón Garcia, A., Brainard, D., Brennan, J., Briones Reyes, B., … Honeycutt, C. W. (2022). Carbon-sensitive pedotransfer functions for plant available water. *Soil Science Society of America Journal, 86, 612-629.* https://doi.org/10.1002/saj2.20395

Bagnall, D. K., Morgan, C. L. S., Bean, G. M., Liptzin, D., Cappellazzi, S. B., Cope, M., Greub, K. L. H., Rielke, E. L., Norris, C. E., Tracy, P. W., Aberle, E., Ashworth, A., Tavarez, O. B., Bary, A. I., Baumhardt, R. L., Gracia, A. B., Brainard, D. C., Brennan, J. R., Reyes, D. B., … Honeycutt, C. W. (2022). Selecting soil hydraulic properties as indicators of soil health: Measurement response to management and site characteristics. *Soil Science Society of America Journal*, 1-21. https://doi.org/10.1002/saj2.20428

Bitterlich M., Franken P., Graefe J. (2018.) Arbuscular Mycorrhiza Improves Substrate Hydraulic Conductivity in the Plant Available Moisture Range Under Root Growth Exclusion. *Frontiers in Plant Science.* Vol. 9. DOI=10.3389/fpls.2018.00301

C. W. Fetter, "Applied Hydrology. 3rd Edition, Prentice Hall," Upper Saddle River, New Jersey, 1994.

Haney, R., Haney, E., Smith, D., Harmel, R., White, M. (2018). The soil health tool-Theory and initial broad-scale application. *Applied Soil Ecology*. Vol 125, 162-168. https://doi.org/10.1016/j.apsoil.2017.07.035

Flynn K., Bagnall D., and Morgan C. (2019). Evaluation of SLAKES, a smartphone application for quantifying aggregate stability, in high-clay soils. *Soil Science Society of America Journal*. https://doi.org/10.1002/saj2.20012

Kemper W., Rosenau R. (1986). Aggregate Stability and Size Distribution. Methods of Soil Analysis: Part 1 https://doi.org/10.2136/sssabookser5.1.2ed.c17

Kleber, M., Christy, I., Myrold, D. (2021) Dilute permanganate oxidizes organic functional groups typically associated with polyphenolic compounds. AGU Meeting Abstracts. https://ui.adsabs.harvard.edu/abs/2021AGUFM.B15M1581K

Leverett, Kelsi T. (2021). Estimation of Soil Hydrologic Parameters and Evaluation of Subsurface Tile Drainage Using Geophysical Techniques. [Doctoral dissertation. Missouri University of Science and Technology].

Liptzin, D., Norris, C., Cappellazzi, S. et al. (2022) An evaluation of carbon indicators of soil health in long-term agricultural experiments. *Soil Biology and Biochemistry*, Vol. 172. 108708, https://doi.org/10.1016/j.soilbio.2022.108708.

Longepierre, M., Widmer, F., Keller, T. *et al.* (2021). Limited resilience of the soil microbiome to mechanical compaction within four growing seasons of agricultural management. *ISME COMMUN.* 1, 44. https://doi.org/10.1038/s43705-021-00046-8

Meter Group. (n.d.) *Environment Products.* https://www.metergroup.com/en/meter-environment/products?UGFyYW1ldGVy=Y20vZA%3D%3D Accessed 10/20/2022.

Mikha M., Rice C. (2004). Tillage and Manure Effects on Soil and Aggregate-Associated Carbon and Nitrogen. *Soil Science Society of America Journal* https://doi.org/10.2136/sssaj2004.8090

Moebius-Clune, B.N., D.J. Moebius-Clune, B.K. Gugino, O.J. Idowu, R.R. Schindelbeck, A.J. Ristow, H.M. van Es, J.E. Thies, H.A. Shayler, M.B. McBride, K.S.M Kurtz, D.W. Wolfe, and G.S. Abawi, 2016. Comprehensive Assessment of Soil Health – The Cornell Framework, Edition 3.2, Cornell University, Geneva, NY.

Nimmo J., Perkins K. (2002). Aggregate Stability and Size Distribution. Methods of Soil Analysis. Part 4 https://doi.org/10.2136/sssabookser5.4.c14

Norris CE, Bean GM, Cappellazzi SB et al. (2020) Introducing the North American project to evaluate soil health measurements. *Agronomy Journal.* 112, 3195-3215. https://doi.org/10.1002.agj2.20234

Rieke, E., Cappellazzi, S., Cope, M. et al. (2022) Linking soil microbial community structure to potential carbon mineralization: A continental-scale assessment of reduced tillage. *Soil Biology and Biochemistry, Vol* 168. 108618, ISSN 0038-0717, https://doi.org/10.1016/j.soilbio.2022.108618.

Sherbine, K., Frankl, A., Fernandez, F., Pease, L., Cates, A. (2023). Haney Soil Health Test changes with season, not subsurface drainage. *Agricultural & Environmental Letters. Vol*. 8, https://doi.org/10.1002/ael2.20098

Schindelbeck, R.R., A.J. Ristow, K.S. Kurtz, L.F.Fennell, H.M. van Es., January 2017. Cornell University Comprehensive Assessment of Soil Health Laboratory Soil Health Manual Series

Silvestrini, R., Burke, S. *Linear Regression Analysis with Jmp and R*. Milwaukee Wisconsin: ASQ Quality Press; 2018.

Singh, S., Jagadamma, S., Yoder, D., Yin, X., Walker, F. (2020) Agroecosystem management responses to Haney soil health test in the southeast United States. *Soil Science Society of America Journal*. *vol*. 84, 1705-1721. https://doi.org/10.1002/saj2.20131

Soil Survey Staff. 2022. Kellogg Soil Survey Laboratory methods manual. Soil Survey Investigations Report No. 42, Version 6.0. U.S. Department of Agriculture, Natural Resources Conservation Service.

Soil Survey Staff, Natural Resources Conservation Service, United States Department of Agriculture. Web Soil Survey. Available online. Accessed 10/20/2022.

Taylor, S. A. and Ashcroft, G. L. (1972) Physical Edaphology- The Physics of Irrigated and Nonirrigated Soils. *Soil Science Society of America Journal*, vol. 38, 1. https://doi.org/10.2136/sssaj1974.03615995003800010002x

USDA Tech Note 450-03: Recommended Soil Health Indicators and Associated Laboratory Procedures

Usowicz, B. and Lipiec, J. (2021). Spatial variability of saturated hydraulic conductivity and its link with other soil properties at the regional scale. *Nature Portfolio,* 11: 8293. https://doi.org/10.1038/s41598-021-86862-3

Wade, J., Maltais-Landry, G., Lucas, D. E., Bongiorno, G., Bowles, T. M., Calderón, F. J., Culman, S. W., Daughtridge, R., Ernakovich, J. G., Fonte, S. J., Giang, D., Herman, B. L., Guan, L., Jastrow, J. D., Loh, B. H. H., Kelly, C., Mann, M. E., Matamala, R., Miernicki, E. A., ... Margenot, A. J. (2020). Assessing the sensitivity and repeatability of permanganate oxidizable carbon as a soil health metric: An interlab comparison across soils. *Geoderma*, *366*, 114235. https://doi.org/10.1016/j.geoderma.2020.114235

VITA

Lyndsey Raymond Bennett was born in Dundee Scotland in 1985 to an active-duty military family. She joined the Air Force in 2006 as an operational weather forecaster. During that time, she earned her associate in applied science in Weather Technology from the Community College of the Air Force before being awarded a Commendation Medal for her duties as a shift supervisor and technical forecasting lead. After four years of service, she received her honorable discharge from active duty in 2010. She continued on to complete her bachelor's degree in general science from Southern New Hampshire University in 2017 and her master's degree in Geological Engineering in May 2023 from Missouri University of Science and Technology.